PHILOSOPHICAL TRANSACTIONS OF THE ROYAL SOCIETY A MATHEMATICAL, PHYSICAL & ENGINEERING SCIENCES

Mechanics of Ship Capsize under Direct and Parametric Wave Excitation

J. M. T. Thompson, R. C. T. Rainey and M. S. Soliman

Phil. Trans. R. Soc. Lond. A 1992 **338**, 471-490
doi: 10.1098/rsta.1992.0015

Mechanics of ship capsize under direct and parametric wave excitation

By J. M. T. Thompson, R. C. T. Rainey† and M. S. Soliman

Centre for Nonlinear Dynamics and its Applications, Civil Engineering Building, University College London, Gower Street, London WC1E 6BT, U.K.

The equations of motion of a ship that is simultaneously heaving, swaying and rolling in waves are derived from first principles in a manner that allows considerable generalization of the sea-state, and offers a systematic approximation of the hydrodynamic pressures by an expansion of the velocity potential in circular harmonics. Assumption of static balance in heave reduces the problem to a single roll equation with both direct and parametric excitation, the latter multiplying the conventional *GZ* restoring function. Numerical steady-state and transient studies of an archetypal biased boat confirm that our earlier conclusions, about basin erosion and the importance of transient capsize, are preserved under realistic magnitudes of parametric excitation.

1. Introduction

The new geometrical phase space techniques of nonlinear dynamics have much to offer the naval architect in his studies of ship dynamics and capsize. In particular it appears that they can be used to establish suitably brief and searching test procedures both for physical model tests and for computational studies. In ship manoeuvring, naval architects have indeed long recognized the usefulness of standard tests such as the 'Dieudonné spiral' and the 'overshoot and zig-zag test' (see, for example, Lewis 1989). We feel that some similar tests are long overdue for the stability of boats against capsize, and the validity of some of our earlier proposals for an 'index of capsizability' based on transient testing is strongly supported by the present work.

A boat in waves is adequately modelled as a rigid body with its six degrees of freedom. Under the beam-sea excitation that is of primary concern here, these can be reduced to the three planar coordinates: while the static balance of the conventional *GZ* approximation reduces the problem to a highly nonlinear one with a single active generalized coordinate. It is precisely for such intrinsically low-dimensional systems that dynamical systems theory can offer its most immediate advantages (Thompson & Stewart 1986).

Our earlier careful studies of an archetypal capsize model (Thompson *et al.* 1990) have indeed already highlighted the new phenomenon of sudden basin erosion by incursive fractals. These show that transient capsize is not only important, but also more predictable than had been previously supposed: allowing fairly precise and logical ideas of a *transient capsize diagram*, and an *index of capsizability* to be

† Permanent address: Atkins Engineering Science, Woodcote Grove, Epsom, Surrey KT18 5BW, U.K.

Phil. Trans. R. Soc. Lond. A (1992) **338**, 471–490
Printed in Great Britain

formulated (Rainey & Thompson 1991). Examination of transients was shown to be conceptually simpler, yet more realistic, than steady-state studies.

Emphasis on transient conditions is therefore a useful paradigm shift in capsize studies, and allows sensible strategies to be mapped out for the very expensive investigations that have to be undertaken by either physical model testing or computer simulation. The latest and most comprehensive experimental (Grochowalski 1989) and computational (De Kat & Paulling 1989) capsize studies certainly point to the urgent need for such brief but searching procedures. Our suggestion that models should be subjected to a short 'worst-case' pulse of regular waves close to the natural roll frequency, rather than long-term stochastic forcing, could for example be a great saver of time and money: especially since the latter often produces no capsize at all (see, for example, Morrall 1981).

In this paper we make a new derivation, from first principles, of an archetypal equation for ship capsize studies. Coupled equations of heave, sway and roll are derived using the Froude–Krilov assumption that the wave pressures are not disturbed by the boat. The acceleration of coordinate axes tied to a circling water particle gives an effective gravitational field $\boldsymbol{g}_{\mathrm{e}}$ perpendicular to the wave surface. The first approximation presented in the main text assumes this surface to be locally straight, above a uniform pressure gradient equal to $\rho \boldsymbol{g}_{\mathrm{e}}$. In the Appendix, expansion of the velocity potential in circular harmonics points the way to a systematic improvement of this approximation. This improvement throws light on the curious lack of direct heave resonance, and allows a discussion of different hull forms, showing for example that the direct forcing term of the first-order canonical equation is exact for a box-shaped hull with a 2:1 aspect ratio.

The assumption of *static balance* in heave leads to a single roll equation which contains implicitly a slave variation (independent of $\boldsymbol{g}_{\mathrm{e}}$) of the heave coordinate. This archetypal equation in the roll angle relative to the wave normal includes both direct forcing (deriving from the rotational acceleration of the wave normal) and parametric excitation (generated by the fluctuating gravitational field). It is particularly valuable because it only involves the conventional GZ function which is the only hull property that routinely appears in the naval literature. This function quantifies the roll response under a pure disturbing moment applied slowly to the boat in still water, during which the static balance is exactly realized, and the passive heave is a major contributor to the potential energy increase of the boat and water.

To assist the reader, the main text presents first the special case of linear surface waves on deep water, before generalizing the derivation to more complex waves, which might typically be in shallow water, oblique to the boat, or indeed nonlinear. In this generalization the forcing magnitudes are expressed in terms of the horizontal and vertical particle accelerations, allowing their absolute, as well as their relative values, to be assessed.

For numerical studies the effective GZ curve of a biased boat is approximated as a quadratic function and related to the escape from a cubic potential well under horizontal and vertical excitation. The archetypal capsize equation, its generalization in §2.7 and its systematic improvements in the Appendix, all have the direct and parametric forcing separated by a 90° phase shift. This is relaxed in some of the computations to explore more general escape and capsize scenarios, revealing an interesting suppression of escape under one form of synchronized forcing.

In these numerical studies we first explore the steady-state response, and the governing bifurcations, in the region of the primary roll resonance. These local

PHILOSOPHICAL TRANSACTIONS OF THE ROYAL SOCIETY A MATHEMATICAL, PHYSICAL & ENGINEERING SCIENCES

bifurcations include the saddle-node folds that give the jumps to and from resonance at the extremities of a hysteresis cycle: the super-critical flip to a subharmonic motion of order two that signals the start of a period-doubling cascade to chaos: and the boundary crisis at which the chaotic attractor finally loses its stability. The bifurcation arcs are drawn in the control space spanned by the magnitudes of the direct and parametric forcing, allowing regions of inevitable capsize to be identified. The unfolding of the transcritical bifurcation encountered under pure parametric excitation serves to organize the diagram, and the subtleties of the indeterminate jumps to resonance are outlined. The inclusion of the parametric forcing means that a biased boat is no longer insensitive to the direction of propagation of beam waves.

Basin erosion studies are made at a relatively high ratio of parametric to direct excitation. This would correspond to a fairly extreme extrapolation of our beam-sea study to a boat almost head-to-sea in very oblique waves, close to the archetypal 'survival mode' for a storm in which the master heads the boat as closely as possible into the waves. The sharp premature loss of the safe basin is still observed under these conditions. So our earlier conclusions about premature, yet predictable, transient capsize are preserved over a wide range of direct plus parametric excitation for critical encounter frequencies close to the roll natural frequency.

2. Derivation of the equations of motion

In this section we derive the equations of motion of a vessel in long beam seas, paying special attention to the coupling action between heave and roll. We are particularly interested in large angles of roll, including, for example, capsize, and are therefore forced to approximate, since the full equations of motion of a vessel, valid for such large motions, are prohibitively complicated. We adopt the standard 'Froude–Krilov' approximation, in which the vessel is assumed not to disturb the water pressure in the waves, but follow it with greater rigour than is customary, identifying first those forces traceable to the spatially invariant (but time varying) part of the pressure gradient, and then (in the Appendix) those forces traceable to its spatial variations. Hydrodynamic forces due to motion of the boat relative to the waves are not considered, so empirical terms must be added to the final equation to incorporate the added hydrodynamic mass and the hydrodynamic damping.

2.1. *Equations of heave, roll and sway in calm water*

Consider first a boat of mass m, moving as a rigid body in calm water with three planar degrees of freedom as shown in figure 1*a*. In the fixed inertial reference frame shown, the centre of gravity of the boat, G, has sway, x, and heave, y, and the roll angle relative to the vertical is θ.

The archimedian upthrust, Rg, equal and opposite to the weight of water displaced, acts vertically through the centre of buoyancy, B. It can be written in terms of W, the volume of water displaced, as

$$R(y,\theta)\,g = \rho g W(y,\theta), \tag{1}$$

where g is the gravitational constant and ρ is the density of the water. We recognize that R and W are functions of y and θ, but not of x. The restoring moment about G, provided by R, can be written in terms of the horizontal distance GZ as

$$M(y,\theta)\,g = R(y,\theta)\,gGZ(y,\theta). \tag{2}$$

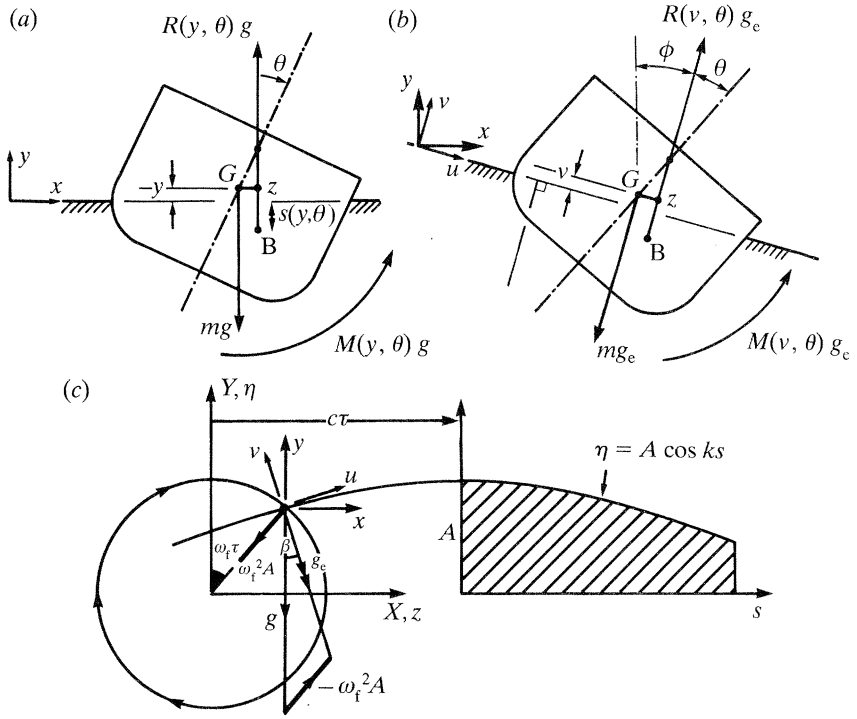

Figure 1. The heave, roll and sway of a boat: (*a*) in calm water; (*b*) in a wave. The mechanics of a linear surface wave on deep water are summarized in (*c*).

The equation of sway motion is given trivially by

$$mx'' = 0, \tag{3}$$

implying that under these hydrostatic forces G would remain on a fixed vertical line, while the coupled equations of heave and roll are

$$my'' + mg - R(y, \theta)\, g = 0, \tag{4}$$

$$I\theta'' + M(y, \theta)\, g = 0. \tag{5}$$

Here a prime denotes differentiation with respect to time, and I is the moment of inertia of the boat about its centre of gravity.

Because the system comprising the boat and ocean is manifestly a conservative mechanical system, the coupled restoring functions are derivable from a potential function. Indeed the internal consistencies of an energy approach make it an attractive analytical tool in deriving the functions for a prescribed hull form. The energy formulation is also invaluable in showing that capsize, in the presence of heaving motions, is entirely analogous to the escape from a two-dimensional potential well corresponding to $V(y, \theta)$.

In general terms, the energy formulation proceeds as follows. In an infinite ocean, the volume of water $W(y, \theta)$ is effectively displaced from its centre of gravity, B, at depth $S(y, \theta)$, to the surface. So the potential energy of the water is

$$U(y, \theta) = \rho g W(y, \theta)\, S(y, \theta) \tag{6}$$

and the total potential energy of the system, boat plus water, is

$$V(y, \theta) = mgy + U(y, \theta). \tag{7}$$

The two restoring functions of (4) and (5) are derivable from V, so the equations can be written formally as

$$my'' + \partial V/\partial y = 0, \tag{8}$$

$$I\theta'' + \partial V/\partial \theta = 0. \tag{9}$$

Notice that it is the vertical movements of the boat and displaced water that provide the restoring moment: the work done in slowly rolling a boat is stored as potential energy of boat and water.

2.2. *The GZ approximation in calm water*

To simplify the coupled heave and roll equations, (4) and (5) of our vectorial derivation, we can assume that we always have vertical *static balance* by setting $y'' = 0$. This is often a good approximation because the heave natural frequency is usually high in comparison with the roll natural frequency: so the heave coordinate can respond quickly to the slower changes in the roll angle, making it a passive slave variable.

Setting $y'' = 0$ in the heave equation, (4), gives us

$$m = R(y, \theta), \tag{10}$$

which we can in principle solve to find the slave relation

$$y = y_s(\theta). \tag{11}$$

The fact that g does not appear in (10) and (11) means that this slave relation will be preserved unchanged when, in our later analysis, a boat in waves experiences a varying effective gravitational field.

Substituting (11) into the roll equation, (5), and writing

$$mgG_z(\theta) \equiv M[y_s(\theta), \theta]g \equiv mgGZ[y_s(\theta), \theta], \tag{12}$$

we have finally the one-degree-of-freedom (G_z) approximation,

$$I\theta'' + mgG_z(\theta) = 0. \tag{13}$$

In using this single roll equation we should always remember that it implies a hidden slave variation of the heave coordinate y to maintain a constant immersed volume $W(y, \theta) = m/\rho$. This passive heave of G is in no way a small correction, but is a major contributor to the form of $G_z(\theta)$ through the substitution of $y_s(\theta)$ in (12). In a vertical-sided vessel, for example, the distance from G to the water surface, measured along the vessel's plane of symmetry, must clearly remain constant, implying a co-sinusoidal rise of G as the boat rolls (a pendulum-like motion, but with no horizontal movement of G). As we have remarked, it is the potential energy of boat and water that generates the restoring moment.

The function $G_z(\theta)$ is the 'GZ characteristic' of the naval literature, and is numerically equal to the distance GZ of figure 1*a*, as we can see in equation (12). But we prefer to introduce a distinctive symbol to emphasize the functional relations involved. In a static test of a ship or model, $mgG_z(\theta)$, would be the pure overturning moment that would be recorded as producing a roll angle of magnitude θ.

2.3. *Surface waves and the effective gravitational field*

Before we proceed to our formulation of boat dynamics in waves, we summarize here some well-known results from the linear theory of surface waves on deep water.

Figure 1*c* shows a sinusoidal surface wave travelling from left to right, the wave height at distance z and time τ being

$$\eta = A\cos(kz - \omega_f \tau) \tag{14}$$

in terms of the wave height A ($2A$ from crest to trough) and the two independent kinematic parameters, the wave frequency, ω_f, and the wavenumber, k. The wave slope is

$$\eta_z(z,\tau) = -Ak\sin(kz - \omega_f \tau) \tag{15}$$

and evaluated at $z = 0$, where our attention will be focused,

$$\eta_z(0,\tau) = Ak\sin\omega_f \tau. \tag{16}$$

By definition, the wave period, T, the wave length, λ, and the wave velocity, c, are

$$T = 2\pi/\omega_f, \tag{17}$$

$$\lambda = 2\pi/k, \tag{18}$$

$$c = \lambda/T = \omega_f/k. \tag{19}$$

Finally the hydrodynamic theory of linear waves on deep water gives us the *dispersal relation*

$$\omega_f^2 = gk. \tag{20}$$

This hydrodynamic result leaves us with just one independent parameter: and we notice that longer waves travel faster.

Now a water particle on the surface stays on the surface, and describes the circle shown. In visualizing this we can imagine a bead rotating around the circle as a wire with the shape $A\cos ks$ is pulled through it with velocity c. Notice that because the wave is assumed to be shallow, all points on the circle can be deemed to have the coordinate $z = 0$.

The centrifugal acceleration of this water particle can be combined vectorially with g to give an effective $\boldsymbol{g}_e$ at the angle β, as shown. Then assuming that $\omega_f^2 A \ll g$ we have

$$\beta \approx (\omega_f^2 A\sin\omega_f \tau)/g = \eta_z(0,\tau), \tag{21}$$

which proves that at any instant of time the effective gravitational force is perpendicular to the water surface.

2.4. *Equations of heave, roll and sway in a wave*

The approach of this heuristic study is to assume that we have a small boat that tracks around the circle of figure 1*c* with the water particle. In doing so it experiences a fluctuating gravitational field that is always perpendicular to the water surface. As a coordinate frame we use the non-rotating axes (x, y), whose origin is tied to the water particle: in such a frame the dynamics will be normal, provided that we recognize the existence of the rotating gravitation field. We shall want to write the buoyancy forces in terms of the rocking axes (u, v), which are always aligned with the water surface: but a dynamic analysis in this frame would be inconvenient due to the large number of extraneous dynamical forces (coriolis, etc.) that would have to be introduced.

We assume that the wave is uninfluenced by the presence of the boat, and in the first instance assume also that the surface can be taken as straight in the vicinity of the boat, with the pressure increasing linearly with distance from it, according to the

current effective $\boldsymbol{g}_e$. This latter assumption follows from the smallness of the boat's cross-section relative to the wave. In the Appendix, we refine our treatment by considering systematically the limiting case of a small boat, and identifying the leading-order terms in the force and moment on it.

Figure 1*b* shows the boat displaced relative to the wave surface, with the coordinate axes displaced to the side for clarity. The normal to the wave surface is inclined at the angle ϕ to the vertical, and θ measures the relative roll.

Relative to the wave, the geometry of this diagram is identical to that of figure 1*a*, with the distance from G to the surface now appearing as v rather than y. We conclude that with just the change in variable from y to v, and the change in gravity from g to the time-varying g_e, the upthrust function R and consequently the moment function M are unchanged from the calm water analysis.

From our previous examination of surface waves we can write immediately

$$\phi = -\eta_z = -Ak \sin \omega_f \tau, \tag{22}$$

$$\phi'' = Ak\omega_f^2 \sin \omega_f \tau, \tag{23}$$

$$g_e \approx g - \omega_f^2 A \cos \omega_f \tau, \tag{24}$$

and in the (x, y) frame the equations of translation of the boat are

$$mx'' + [m - R(v, \theta)]\, g_e(\tau) \sin \phi = 0, \tag{25}$$

$$my'' + [m - R(v, \theta)]\, g_e(\tau) \cos \phi = 0, \tag{26}$$

whereas the rotational equation

$$I(\phi'' + \theta'') + M(v, \theta)\, g_e(\tau) = 0 \tag{27}$$

becomes on using (23)

$$I\theta'' + M(v, \theta)\, g_e(\tau) = -IAk\omega_f^2 \sin \omega_f \tau. \tag{28}$$

These equations involving a mixture of (x, y) and (u, v) coordinates are not suitable for immediate use, but allow us to proceed to a one-degree-of-freedom simplification along the lines of the calm water analysis.

2.5. *The GZ approximation in waves*

Static balance is achieved simultaneously in the x and y directions by setting $m = R(v, \theta)$, in equations (25) and (26). Notice that since the effective gravity influences the boat and water equally, this static balance condition, and the resulting slave relation

$$v_s = v_s(\theta) \tag{29}$$

are exactly the same as in the calm water analysis. Substituting (29) into (28) gives

$$I\theta'' + M[v_s(\theta), \theta]\, g_e(\tau) = -IAk\omega_f^2 \sin \omega_f \tau \tag{30}$$

and finally, using (24), we have the one-degree-of-freedom equation of rolling motion

$$I\theta'' + mgG_z(\theta)[1 - (\omega_f^2 A/g) \cos \omega_f \tau] = -IAk\omega_f^2 \sin \omega_f \tau. \tag{31}$$

A valuable generalization of these equations is given in §2.7 as equations (30*a*) and (31*a*). The equations have direct rolling excitation on the right-hand side, and parametric forcing on the left. The formulation is particularly useful because it only involves the known calm-water $G_z(\theta)$ function that appeared in (13): this is the only hull property that routinely appears in the naval literature.

2.6. *Canonical roll equation with parametric excitation*

To tie in with our earlier studies of direct excitation, we now adopt the simplest possible restoring moment; assuming, as appropriate for a generic and worst case analysis, that the boat is biased by wind, ice or cargo imbalance. With θ now measured from the (positive) tilted equilibrium state, we write the total effective restoring moment, comprising the original GZ characteristic plus the biasing moments, as

$$mgG_z(\theta) = c\theta[1-(\theta/\theta_{\mathrm{v}})], \tag{32}$$

where c is the linear stiffness and θ_{v} is the angle at which the moment vanishes, the 'angle of vanishing stability'. Notice that this quadratic restoring function implies that the biasing acts so strongly towards positive θ that there is no possibility of capsize in the negative θ direction: this is physically reasonable for a vessel subjected to lateral wind loading.

The natural frequency of the boat, in the real time τ, is ω_n, with $\omega_n^2 = c/I$. We now scale the time so that $\omega_n \tau \equiv t$, using a dot to denote differentiation with respect to t, and scale the angle so that $\theta/\theta_{\mathrm{v}} \equiv x$. This notation agrees with our previously published work, and it is felt that there can be no possible confusion between this x and the one used in earlier sections as a coordinate axis. Defining also the new parameters

$$\omega \equiv \omega_{\mathrm{f}}/\omega_n, \tag{33}$$

$$F \equiv -Ak\omega^2/\theta_{\mathrm{v}}, \tag{34}$$

$$G \equiv -A\omega_{\mathrm{f}}^2/g = -Ak, \tag{35}$$

the final canonical equation of motion is

$$\ddot{x} + \beta\dot{x} + x(1-x)\,[1 + G\cos wt] = F\sin\omega t. \tag{36}$$

Here we have inserted an arbitrary linear damping term with coefficient β, corresponding to a damping ratio of $\zeta = \frac{1}{2}\beta$. This equation is preserved in our generalized analysis of §2.7, subject to (34) and (35) being replaced by (34a) and (35a) of that section. The ratio of the forcing magnitudes in (36) is

$$G/F = \theta_{\mathrm{v}}/\omega^2. \tag{37}$$

The angle of vanishing stability, θ_{v}, will be of the order of one radian, and if we are studying primary resonance the frequency ratio ω of (33) will be of order unity. So we conclude that G and F will be of the same order of magnitude. Their absolute magnitudes are discussed in the last paragraph of §2.7.

2.7. *Generalization to nonlinear, oblique and shallow-water waves*

The above analysis has been restricted to linear waves on deep water for simplicity of presentation, but in fact the argument is much more general. This is because the key result is that established at the end of §2.3, namely that the effective gravitational force vector, $\boldsymbol{g}_{\mathrm{e}}$, is perpendicular to the water surface. It is this which allows the still-water hydrostatic arguments to be applied in §2.4, with the magnitude of the vector, g_{e}, replacing g.

That the effective gravitational force is perpendicular to the wave surface can, however, be seen to be true in general, from first principles. This is because the water surface is a constant-pressure contour (the pressure being atmospheric there), so the

PHILOSOPHICAL TRANSACTIONS OF THE ROYAL SOCIETY A MATHEMATICAL, PHYSICAL & ENGINEERING SCIENCES

pressure gradient in the water must be normal to the surface. The fundamental Euler equation of an ideal fluid (see, for example, Lighthill 1986, §3.3) equates the pressure gradient to the particle acceleration, including gravity. So vector $\boldsymbol{g}_e$, which is related by definition to the total particle acceleration, is always perpendicular to the water surface, no matter how complex the wave.

Following the argument of §§2.4 and 2.5 for this more general case, we see that equation (30) can be written more generally, using (12), as

$$I\theta'' + mg_e(\tau)\, G_z(\theta) = I\eta_z'', \tag{30a}$$

where $g_e(\tau)$ is the magnitude of the effective gravity vector, and η_z is the wave slope. Written in this very general way, the equation can be used for a wide variety of waves, including steep, nonlinear ones.

Now thinking in terms of a generalization of the gravity vectors and particle accelerations of figure 1*c* we can write some approximate equalities as follows. Horizontal component of the particle acceleration $\approx A_h \sin\omega_f\tau \approx g\eta_z$. Vertical component of the particle acceleration $\approx A_v \cos\omega_f\tau \approx g - g_e(\tau)$. We can use these to express the excitations in terms of the particle accelerations, to give us the generalization of (31),

$$I\theta'' + mgG_z(\theta)[1 - (A_v/g)\cos\omega_f\tau] = -(IA_h\omega_f^2/g)\sin\omega_f\tau. \tag{31a}$$

This can be reduced to the canonical form (36) by modifying the definitions of F and G as follows

$$F = A_h\omega^2/g\theta_v, \tag{34a}$$

$$G = A_v/g, \tag{35a}$$

giving

$$G/F = A_v\theta_v/A_h\omega^2. \tag{37a}$$

The 90° phase difference between the direct and parametric excitation is seen to be preserved in the generalization of (36). It follows from the 90° phase difference between the components of the particle accelerations, which is a consequence of one being in phase with the wave slope, and the other in phase with the wave elevation.

In linear deep-water waves the particle orbits are circular with $A_v = A_h$ so that (37*a*) degenerates to (37) implying that G/F is approximately unity as observed earlier. However, the present more general treatment reveals the types of waves which will produce other values for G/F.

First, for G/F to be less than unity, we require A_h to be larger than A_v, implying that the particle orbits are horizontally elongated ellipses. This situation arises in shallow water.

Conversely, for G/F to be greater than unity we require the orbits to be vertically elongated ellipses. This situation arises if the ship is not in beam waves, but in oblique waves, so that an observer looking down the length of the hull would only see a component of A_h. This second scenario is clearly less precise than the first, because in oblique waves the ship will pitch as well as roll, introducing extra degrees of freedom into the problem. However, the two cases do establish in broad outline the scenario sketched in figure 2.

It remains to quantify the range of possible magnitudes for F and G, which for our case of θ_v/ω^2 close to unity, can be seen to be approximately A_h/g and A_v/g respectively. These are well known to be limited to about 0.5, with the important proviso that once a wave breaks the horizontal acceleration on the vertical face just beneath the crest can be much higher, typically $5g$ (New *et al.* 1985).

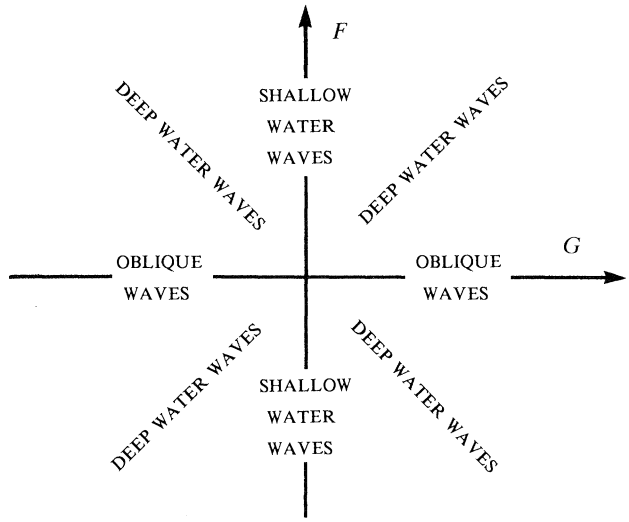

Figure 2. Regions of the (F, G) control space corresponding to some generalized scenarios.

2.8. *Source of excitation and lack of heave resonance*

The parametric forcing derives from the fluctuating gravitational field experienced by the boat and water as they follow the circular path of a water particle. Since the time-varying $\boldsymbol{g}_e$ effects the boat and water equally, it induces no pure heave response: and the slave, roll-induced heave, has the calm-water form $y_s(\theta)$.

This lack of any heave resonance follows from the absence of g from equation (10). It can be established most clearly by considering a symmetric boat floating in a container that is given an up–down sinusoidal oscillation with no horizontal translation. The hydrostatic pressures respond instantaneously to the sinusoidally fluctuating g_e, so the resultant force on any body will be just as needed to keep the displaced water at rest in a coordinate frame tied to the container. So the archimedian upthrust on a displaced volume, W, still acts through the centre of gravity of W and has the magnitude $\rho g_e W$. As far as the hydrostatic forces of our present study are concerned, the equations of motion of the boat in the sinusoidally elevated container are just those of the calm water analysis, (3), (4), (5) and (13), with g replaced by $g_e(\tau)$. With no roll, the boat floats in equilibrium at its usual depth in the water, $y_s(0)$: there is no heave relative to the container, and no pure heave resonance can be excited. This analogy with a boat in a container does of course not address the non-uniform pressure gradients that are examined more carefully in the Appendix, where it emerges that in waves short enough to cause heave resonance they will produce a heave excitation of the same order as the other terms in the heave equation.

With our use of the relative angle θ, which appears in the GZ restoring functions, the direct forcing derives from the rotational acceleration of the wave surface. Contrasting this direct roll forcing with the lack of heave excitation gives us the suspicion of a contradiction here. For if we were to consider a boat with two slender parallel hulls (i.e. a catamaran), and apply the above heave argument to each of them individually, we would conclude that each would track the water surface, and thus that there was no roll excitation F on the catamaran as a whole. This paradox clearly arises from treating two hulls of the catamaran separately, and recognizing a slight

phase difference in the two heave forces. In doing so we are implicitly modelling the pressure field to a higher degree of approximation than before. By introducing a systematic approximation scheme, these and other anomalies are resolved in the Appendix.

To examine the signs of the forcing terms we look again at figure 1*c*. At $t = 0$ the boat is on a crest, and g_e is at a minimum. This is consistent with (36) with G negative as implied by (35). If the wave is propagating to the right, as in the analysis, then one quarter of a cycle later, at $t = +\pi/2\omega$, the surface will have its minimum clockwise rotation, and the direct excitation will be minimum. This is consistent with (36) with F negative as implied by (34).

If the direction of wave propagation is reversed, the sign of F will be reversed, but not the sign of G. Notice that reversing F and G simultaneously has no significance, being just equivalent to a phase shift.

Now our bias implies clockwise capsize, so if this were due to wind, the wind would be from the left. So we have the result, and useful memory aid, that wind and wave travelling in the *same* direction implies that F and G have the *same* sign: wind and wave travelling in the *opposite* direction implies that F and G have the *opposite* sign. The fact that a biased boat is no longer insensitive to the direction of propagation of the beam waves is a new feature that arises once we include the parametric excitation terms.

2.9. *Analogy with a ball rolling in a potential well*

It is useful to relate capsize to the escape from a potential well. Suppose axes (x, y) are tied to a cubic well, and their origin, Q, is given prescribed sinusoidal displacements relative to a fixed frame (X, Y). We write the displacements of the well in the X and Y directions as

$$D_x = -a \sin \omega t, \tag{38}$$

$$D_y = b \cos (\omega t + \psi). \tag{39}$$

To an observer in the (x, y) frame the excitation forces on a mass m are

$$E_x = -m\ddot{D}_x = -ma\omega^2 \sin \omega t, \tag{40}$$

$$E_y = -m\ddot{D}_y = mb\omega^2 \cos (\omega t + \psi). \tag{41}$$

We consider a particle of mass m sliding without friction (or a small ball rolling with negligible rotational inertia) under gravity, g, on the shallow curve given by

$$y = [\tfrac{1}{2}x^2 - \tfrac{1}{3}x^3]/g, \tag{42}$$

$$\mathrm{d}y/\mathrm{d}x \equiv y_x = (x - x^2)/g, \tag{43}$$

for which we have the approximate equation of motion,

$$m\ddot{x} + (mg - E_y)\, y_x = E_x, \tag{44}$$

giving

$$\ddot{x} + \beta\dot{x} + (x - x^2)\,[1 - (b\omega^2/g) \cos (\omega t + \psi)] = -a\omega^2 \sin \omega t, \tag{45}$$

where we have inserted an arbitrary viscous damping term.

If we set $\psi = 0$ we retrieve our canonical capsize equation (36) under the cos/sin forcing with F and G of the same sign, and we observe that this corresponds to the origin of the well, Q, circling anti-clockwise on an ellipse. If we set $\psi = \pi$ we again retrieve (36) under the cos/sin forcing with F and G now of opposite sign, and Q circling clockwise on an ellipse.

PHILOSOPHICAL TRANSACTIONS OF THE ROYAL SOCIETY A MATHEMATICAL, PHYSICAL & ENGINEERING SCIENCES

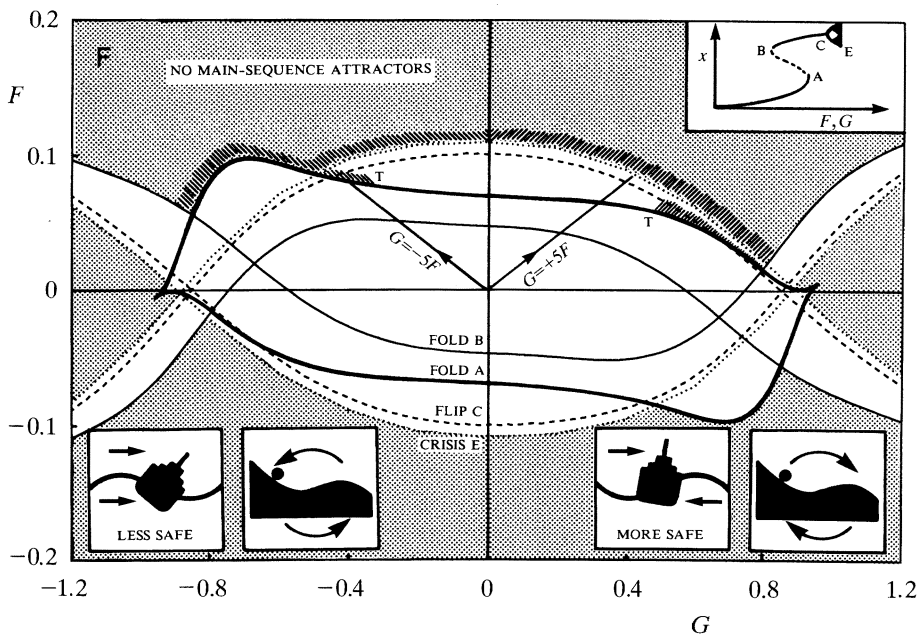

Figure 3. Bifurcations governing the capsize of a biased boat under direct and parametric excitation, based on equation (36) with $\beta = 0.1$ and $\omega = 0.85$. The dot screen indicates the area of no main-sequence attractor. The hatching denotes escape under the slow evolution of the parameters from the origin: the limits of indeterminacy, T, are purely schematic.

Because it gives rise to a new phenomenon of escape suppression, which might be relevant to boats in cross seas, as discussed in §3.3, it will be of interest to explore numerically the behaviour of the equation

$$\ddot{x} + \beta\dot{x} + (x - x^2)[1 + G\sin\omega t] = F\sin\omega t. \tag{46}$$

Notice that setting $\psi = \frac{1}{2}\pi$ in (45) retrieves this sin/sin equation with F and G of opposite sign, corresponding to Q translating on a line whose slope, b/a, is positive. Setting $\psi = \frac{3}{2}\pi$ retrieves this sin/sin equation with F and G of the same sign, corresponding to Q translating on a line whose slope, $-b/a$, is negative.

3. Bifurcation diagrams and integrity curves

We present now some preliminary numerical studies of the canonical capsize equation (36) and its sin/sin complement (46).

3.1. *Steady-state capsize under direct and parametric forcing*

The steady state response of (36) with $\beta = 0.1$ and $\omega = 0.85$ is summarized in figure 3. Starting at rest in the equilibrium condition $F = G = x = \dot{x} = 0$, the system under slowly increasing F and G, say along a ray $G = \alpha F$, will experience a response similar to that of the inset, where x is stroboscopically sampled at the forcing frequency. Here we have a jump to resonance at the saddle-node fold A forming a hysteresis cycle with the jump from resonance at fold B. The resonant harmonic solution starts a period-doubling cascade to chaos at the flip bifurcation C, and the resulting chaotic attractor finally loses its stability at a crisis at E. This crisis can be approximately located by the valuable new Birkhoff-signature technique described by McRobie (1992). The main diagram showing the locus of these bifurcations is unchanged by a

PHILOSOPHICAL TRANSACTIONS OF THE ROYAL SOCIETY A MATHEMATICAL, PHYSICAL & ENGINEERING SCIENCES

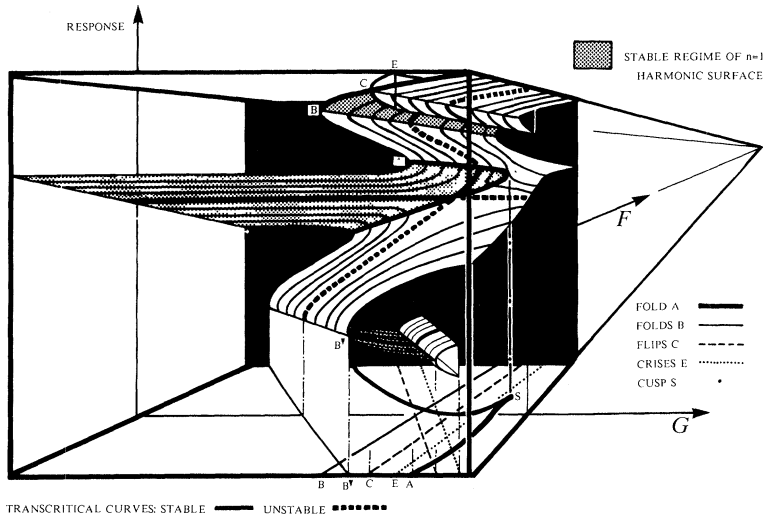

Figure 4. Schematic response surface of the transcritical bifurcation under parametric excitation of magnitude G unfolded by the addition of direct excitation of magnitude F. The stable regime of the $n = 1$ harmonic surface is indicated by the dot screen. The bifurcations on the surface project into the (F, G) control space in the base plane. This bifurcation, and the neighbouring cusp S, organize the fold arcs, A and B of figure 3. (Here B$^{\blacktriangledown}$ identifies the front face.)

180° planar rotation, corresponding to the invariance of (36) under $F, G \to -F, -G$: and the superimposed boats and wells remind us of the physical excitations that correspond to the two distinct quadrants.

Under pure parametric excitation, with $F = 0$, the equilibrium state $x = \dot{x} = 0$ is always a solution but exhibits the well-known Mathieu instability which here corresponds to the *trans-critical* bifurcation sketched in figure 4. This is unfolded by small F as shown, the unfolding serving to organize the bifurcation diagram of figure 3. For a symmetric, unbiased vessel this transcritical bifurcation would of course be replaced by a symmetric one, with the subsequent response exhibiting a symmetry-breaking instability as is observed in the parametrically excited pendulum (Capecchi & Bishop 1990).

In the dotted outer region of figure 3 there are no attractors of the main sequence, so ignoring the highly localized attractors with very small basins that can be expected occasionally beyond E, capsize will be inevitable once we hit this region. There is, however, some possibility of steady-state capsize before this. As we have shown recently for the case of $G = 0$ at lower ω, the jump to resonance can be indeterminate (Thompson & Soliman 1991; Stewart & Ueda 1991) due to saddle-node A lying on a fractal basin boundary.

In the light of this, we have shown by hatching the boundaries at which we would expect steady-state capsize. At the present $\omega = 0.85$, we know from earlier studies at $G = 0$ that on the F axis fold A is determinate and safe, in the sense that the jump to resonance will always restabilize on the fundamental resonant oscillation between B and C. Capsize will subsequently occur at the jump from crisis E. Meanwhile, at the large left-hand bulge of arc A, where $G \approx -9F$, the jump from A is determinate and unsafe with a guaranteed jump out of the potential well to large x and capsize.

Indeterminate jumps from fold A can be expected when E is close to, but beyond A, giving us the hatched regions terminating at points T. These points correspond to

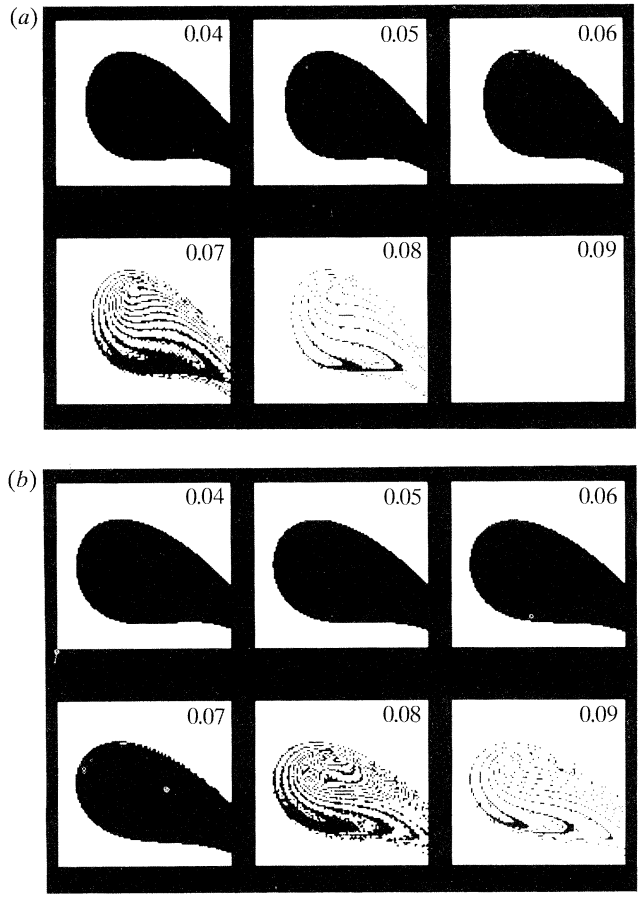

Figure 5. Erosion of the safe basin of non-capsizing starts for equation (36) with $\beta = 0.1$ and $\omega = 0.85$. Each portrait has the abscissa $-0.8 < x(0) < 1.2$ and the ordinate $-1.0 < \dot{x}(0) < 1.0$. Sequence (*a*) corresponds to the control ray $G = 5F$, sequence (*b*) to the ray $G = -5F$. All values indicated are F.

global bifurcations at which there is a heteroclinic tangency between the resonant saddle and the hill-top saddle: they have not been located in the present investigation, and their positions on the diagram are purely schematic. Escape in the vicinity of the G axis is likewise unexplored.

The asymmetry of figure 3, and in particular the left hand bulge of fold A, implies that a biased boat capsizes more easily under steady state conditions if F and G are of the same sign, corresponding to wind and wave in the same direction.

3.2. *Transient capsize under direct and parametric forcing*

We have emphasised in earlier papers (Rainey *et al.* 1990, 1991; Thompson *et al.* 1990; McRobie & Thompson 1990; Thompson 1991) that naval architects should pay more attention to capsize under transient, rather than steady-state conditions. A short train of regular waves close to the roll frequency can be seen as a worst-case excitation scenario: and the rapid erosion of the safe basin of attraction at a well-defined wave magnitude suggests that this could be used to define a valuable 'index of capsizability' for a hull form. The results can be usefully summarized on a *transient*

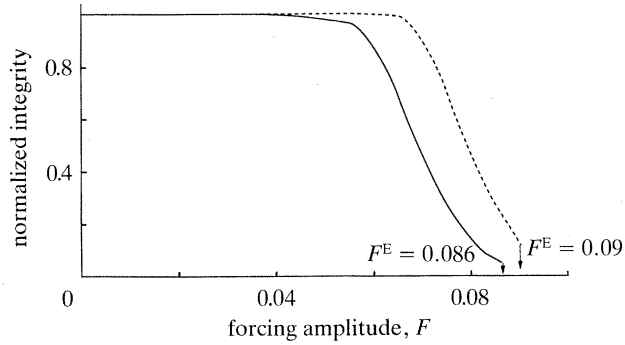

Figure 6. Integrity diagrams showing the variation of the normalized area of the safe basin for the two loading rays of figure 5. Steady-state capsize, corresponding to the final crisis E, would occur at the values of F^{E} indicated. ——, $G = +5F$; – – – –, $G = -5F$.

capsize diagram (Rainey & Thompson 1991) showing the régime of potential capsize on a graph of wave height against wave frequency.

The conclusions of these earlier studies were shown to be robust against the precise forms of the damping and GZ characteristics (Lansbury & Thompson 1990; Soliman 1990; Soliman & Thompson 1991), but no examination has yet been made of the effect of additional parametric excitation. For this reason it is of interest to examine the safe basins of attraction of equation (36) as we simultaneously increase G and F.

Figure 5 shows the evolution of the safe basin as the excitation is increased along the two rays of figure 3: figure 5*a* for $G = +5F$, and 5*b* for $G = -5F$. The abscissa of each phase portrait is the initial value of the coordinate, $x(0)$, and the ordinate is the initial value of its velocity, $\dot{x}(0)$. Starts in the black basin settle onto one or more safe finite attractors leaving the boat in a condition of steady-state rolling, while starts in the white lead to capsize. The sudden striation of the safe basin corresponds to the phenomenon of basin erosion by incursive fractals that we discovered in our earlier work under direct excitation (Thompson 1989; Thompson & Soliman 1990). Subsequent basin erosion studies of ship capsize have been made by Falzarano *et al.* (1992) and Kan *et al.* (1990, 1991). General descriptions of fractal basin boundaries are given by McDonald *et al.* (1985) and Moon (1987): and our recent studies have gone a long way towards explaining the sudden erosion in terms of a heteroclinic tangling of invariant manifolds (Soliman & Thompson 1992).

Plotting the area of the safe basin, normalized to unity at $F = 0$, gives the integrity diagrams (Soliman & Thompson, 1989) of figure 6. These preserve the 'Dover cliff' form of our earlier investigations, showing that our previous conclusions hold good for the very extreme conditions (heading into very oblique waves, for example) implied by the strong parametric excitation of $G = \pm 5F$.

3.3. *Escape from a potential well under direct and parametric forcing*

Figure 7 shows the bifurcation diagram for the sin/sin equation (46) which contrasts markedly with the corresponding figure 3 for the cos/sin equation (36). Once again there is invariance under $F \to -F$, $G \to -G$, and the sketched wells identify the forcing features of the two distinct quadrants. It is particularly interesting to observe that it is very difficult to make the particle escape from the well by vibrating it along a negative gradient, corresponding to F and G having the same sign. Along the ray $G = 5F$, for example, there is no steady-state escape in the region covered by this diagram (Soliman 1992).

PHILOSOPHICAL TRANSACTIONS OF THE ROYAL SOCIETY A MATHEMATICAL, PHYSICAL & ENGINEERING SCIENCES

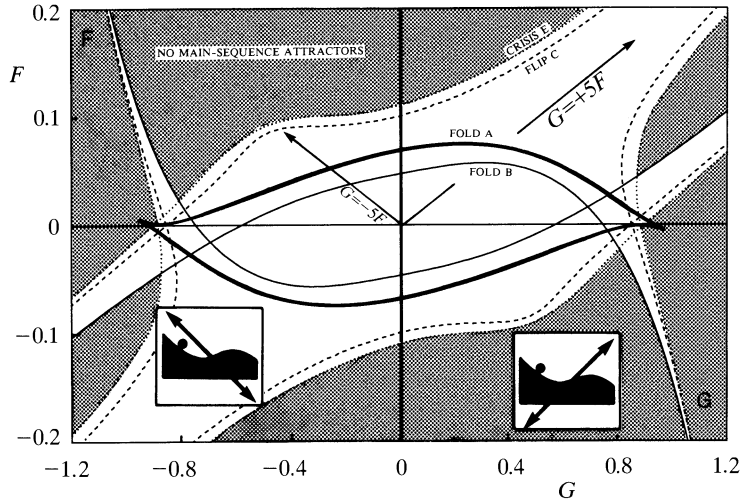

Figure 7. Bifurcations governing the escape from a cubic potential well under direct and parametric excitation, based on equation (46) with $\beta = 0.1$ and $\omega = 0.85$. The dot screen indicates the area of no main-sequence attractor.

This interesting suppression of escape under direct and parametric forcing is being examined in current research. Although it is not observed in the case of cos/sin forcing, it may arise once this 90° phase separation is relaxed. Such a relaxation would be experienced by a boat in cross-seas. If, for example, the boat encountered two wave trains, one beam-on, and one head-on, the latter would provide parametric excitation only, at any arbitrary phase to the beam excitation.

J.M.T.T. gratefully acknowledges the award of a Senior Fellowship by the Science and Engineering Research Council of the United Kingdom.

Appendix. A systematic approximation scheme

The formulation in §2 assumes that the water surface in the vicinity of the boat is straight and the pressure rises linearly with distance from it: the pressure gradient, in other words, is assumed to be everywhere the same ($\boldsymbol{g}_e$), in both magnitude and direction. This is intuitively a good first-order approximation for our case of a boat of small cross-section. In this Appendix we explore that approximation systematically, by retaining the true spatial variations in the pressure gradient, and evaluating the leading order terms in the force and moment on the hull, in the limiting case of small boat cross-section.

A 1. *The pressure equation*

The uniform pressure-gradient $\boldsymbol{g}_e$ is the first term in the full pressure expression

$$\rho[\boldsymbol{g}_e \cdot \boldsymbol{x} - \partial\phi/\partial t - 0.5\nabla\phi \cdot \nabla\phi]$$

where $\boldsymbol{x}$ is a position relative to the boat and $\nabla\phi$ is the water velocity (in the absence of the boat, of course), as seen in our non-rotating (x, y) reference frame moving with a water particle on the surface at the boat's location, at which point $\phi = \nabla\phi = 0$. Notice that in this Appendix we use the conventional symbol ϕ for the velocity potential, there being here no confusion with its earlier use as the wave slope.

PHILOSOPHICAL TRANSACTIONS OF THE ROYAL SOCIETY A MATHEMATICAL, PHYSICAL & ENGINEERING SCIENCES

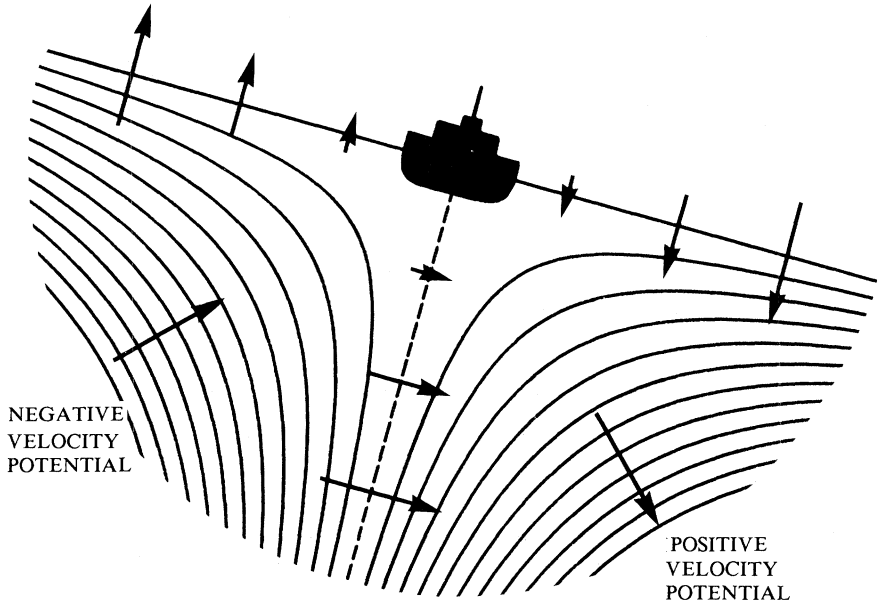

Figure 8. Contours of the velocity potential and the flow field in the 'rocking mode' generated by the circular harmonic $\phi = r^2 \sin 2\theta$.

That this classical irrotational-flow pressure formula holds in our unusual unsteadily accelerating reference frame may be seen from its derivation given by Lighthill (1986) in his §6.1. The frame acceleration $\boldsymbol{g}_e$ merely adds to his equation (175) and transforms the absolute velocity there to the velocity seen in the accelerating frame. The subsequent argument then proceeds unchanged, and $\boldsymbol{g}_e$ emerges as above from his equation (178), with Lighthill's arbitrary constant f being zero by choice of $\phi = 0$ at the location of the boat.

A 2. *Rocking and bending modes*

To proceed with the systematic approximation scheme, we expand the velocity potential ϕ in the standard manner as an infinite series of circular harmonics (Batchelor 1967, equation 2.10.5), with origin at the boat. Successive harmonics give potentials which grow with successively higher powers of distance from the boat, and thus allow the leading order terms in the force and moment on it to be identified, in the limiting case of small boat cross-section. The two lowest-order circular harmonics are those of the second degree (given that $\phi = \nabla\phi = 0$ at the origin), and, if they are aligned with the water surface at the boat at all times, describe respectively the *rocking* and *bending* of the surface.

The rocking mode, given in polar coordinates by $\phi = r^2 \sin 2\theta$, is illustrated in figure 8, where the arrows show the water velocity (as seen in our moving reference-frame, of course), and the contours are those of the velocity potential, ϕ. The bending mode is exactly the same, but rotated through 45°, so that the velocity at the surface is tangential to it. Now the velocities increase with the distance from the boat, and the velocity potentials with the square of the distance, so from the above equation, the pressure must also increase with the square of the distance.

Table 1. *Powers of the boat's beam in the terms of the equations of motion. The extra terms derived in the Appendix are shown in brackets*

	inertia	stiffness	parametric excitation	direct excitation	roll coupling
roll	4th	3rd	3rd (4th)	4th (4th)	—
heave	3rd	2nd	2nd (3rd)	— (3rd)	2nd

A 3. *Orders of the roll moments*

It follows that the roll moment produced will be proportional to the *fourth power* of the beam of the boat: twice for this basic pressure-law, once for the wetted length of hull circumference, and once for the lever arm. Moreover, since the pressure fields are partly port-starboard symmetric, and partly antisymmetric, the excitation will be both parametric and direct, as shown in the first row of table 1, which gives the order of the existing terms in the roll equation, for comparison.

As can be seen, the new terms (shown bracketed) are of the same order in the boat's beam as the existing ones, and so cannot be ignored in the limiting case of small boat cross-section. Unless, that is, the limiting process is taken so far that third-order terms dominate the fourth-order ones. But that would imply that inertia forces were negligible compared with stiffness forces, in other words that the boat is so small that its roll period is much less than the wave period. Since we are assuming the two periods to be comparable, we are implicitly not carrying the limiting process that far, and thus need to retain both third and fourth order terms.

A 4. *Relative phasing of the excitations*

In view of the importance of the phasing of the direct and parametric excitation, established in §3.3, it is interesting to consider the phasing of the new excitation terms. In small waves the dominant pressure term will be that proportional to ϕ, from the $\partial\phi/\partial t$ term in the above equation, because it is directly proportional to waveheight, whereas the other terms are proportional to waveheight squared. Thus in small waves the rocking mode produces a port–starboard antisymmetric pressure field and thus a direct roll excitation, whereas the bending mode produces a port–starboard symmetric pressure field and a parametric roll excitation (and a surface curvature, caused by higher-order water motions allowing the large hydrostatic pressure-gradient to cancel the surface pressure anomaly).

Now the rocking velocity is at a peak at a wave crest or trough, and thus the associated pressure is at a peak at maximum wave slope. The bending velocity, on the other hand, is at a peak at maximum wave slope, and thus its associated pressure is at a peak at a wave crest or trough. This is also true of the existing direct and parametric excitation terms, so the new excitations exactly preserve the crucial 90° phase difference.

A 5. *Effect of the hull form*

It is also interesting to see how the new direct excitation compares with the existing one, for various hull forms. Wide, shallow-draught forms will clearly follow the water surface most closely (since they are effectively getting the same treatment as the surface layer of water particles), implying that the new direct excitation term is then cancelling the existing one. When the beam is reduced to twice the draught, a box-section hull (or indeed a semicircular one) gets zero direct excitation from our

PHILOSOPHICAL TRANSACTIONS OF THE ROYAL SOCIETY A MATHEMATICAL, PHYSICAL & ENGINEERING SCIENCES

new pressure fields by symmetry, so the existing direct excitation term is unaffected. When the beam is much less than the draught, the new direct excitation term changes sign, and so must augment, rather than cancel, the existing one.

A 6. *Orders of the heave forces*

The second row of table 1 gives the order of the terms in the heave equation, to which similar arguments apply, except that heave has the dimensions of length, unlike roll, so that for comparison it is necessary to consider heave in relation to beam, rather than heave itself. This puts an extra power of the beam in the inertia, stiffness, and parametric excitation terms.

As can be seen, the new terms are again comparable with the old ones, just as in roll. This time, however, we are applying a 'static balance' assumption (see §2.5), which requires the dominance of stiffness terms over inertial ones, and is thus neatly met by allowing the limiting process to go far enough for second-order terms to dominate over third-order terms. If this is done, then the new terms can be seen to be immaterial.

The dominance of heave stiffness over heave inertia is equivalent to the heave excitation being at frequencies well below heave resonance. Thus once the excitation frequencies become comparable with the heave resonant frequency, it is no longer justifiable to ignore third-order terms, and thus in particular no longer justifiable to take the heave excitation as zero, which it would be to second order.

References

Batchelor, G. K. 1967 *An introduction to fluid dynamics*. Cambridge University Press.

Capecchi, D. & Bishop, S. R. 1990 Periodic and non-periodic responses of a parametrically excited pendulum. *DISAT Pub. no. 3*. Dipartmento di Ingegneria delle Strutture delle Acque e del Terreno, University di L'Aquila, Italy.

De Kat, J. O. & Paulling, J. R. 1989 The simulation of ship motions and capsizing in severe seas. *Trans. Soc. Naval Archs Marine Engrs* **97**, 139–168.

Falzarano, J. M., Shaw, S. W. & Troesch, A. W. 1992 Application of global methods for analysing dynamical systems to ship rolling motion and capsizing. *Int. J. Bifurcation Chaos*. (In the press.)

Grochowalski, S. 1989 Investigation into the physics of ship capsizing by combined captive and free running model tests. *Trans. Soc. Naval Archs Marine Engrs* **97**, 169–212.

Kan, M., Saruta, T., Taguchi, H., Yasuno, M. & Takaishi, Y. 1990 Model tests on capsizing of a ship in quartering waves. In *Proc. Fourth Int. Conf. on Stability of Ships and Ocean Vehicles* (ed. P. Cassella), vol. 1, pp. 109–116. University of Naples.

Kan, M. & Taguchi, H. 1991 Chaos and fractal in capsizing of a ship. In *Proc. HADMAR 91*. Varna, Bulgaria. (Submitted.)

Lansbury, A. N. & Thompson, J. M. T. 1990 Incursive fractals: a robust mechanism of basin erosion preceding the optimal escape from a potential well. *Phys. Lett.* A **150**, 355–361.

Lewis, E. V. (ed.) 1989 *Principles of naval architecture*, vol. 3 (Motions in waves and controlability). New York: Society of Naval Architects and Marine Engineers.

Lighthill, M. J. 1986 *An informal introduction to theoretical fluid mechanics*. Oxford: Clarendon Press.

McDonald, S. W., Grebogi, C., Ott, E. & Yorke, J. A. 1985 Fractal basin boundaries. *Physica* D **17**, 125–153.

McRobie, F. A. 1992 Birkhoff signature change: a criterion for the instability of chaotic resonance. *Phil. Trans. R. Soc. Lond.* A **338**, 557–568. (This issue.)

McRobie, F. A. & Thompson, J. M. T. 1990 Chaos, catastrophes and engineering. *New Sci.* **126**, 41–46. (9 June 1990.)

Moon, F. C. 1987 *Chaotic vibrations: an introduction for applied scientists and engineers*. New York: Wiley.

Morrall, A. 1981 The *GAUL* disaster: an investigation into the loss of a large stern trawler. *Trans. R. Inst. Naval Arch.* **123**, 391–440.

New, A. L., McIver, P. & Peregrine, D. H. 1985 Computations of overturning waves. *J. Fluid. Mech.* **150**, 233–251.

Rainey, R. C. T. & Thompson, J. M. T. 1991 The transient capsize diagram – a new method of quantifying stability in waves. *J. Ship Res.* **35**, 58–62.

Rainey, R. C. T., Thompson, J. M. T., Tam, G. W. & Noble, P. G. 1990 The transient capsize diagram – a route to soundly-based new stability regulations. In *Proc. Fourth Int. Conf. on Stability of Ships and Ocean Vehicles* (ed. P. Cassella), vol. 2, pp. 613–619. University of Naples.

Soliman, M. S. 1990 An analysis of ship stability based on transient motions. In *Proc. Fourth Int. Conf. on Stability of Ships and Ocean Vehicles* (ed. P. Cassella), vol. 1, pp. 183–190. University of Naples.

Soliman, M. S. 1992 Steady state bifurcations and basins of attraction in a nonlinear system subjected to combined external and parametric excitation. *J. appl. Mech.* (Submitted.)

Soliman, M. S. & Thompson, J. M. T. 1989 Integrity measures quantifying the erosion of smooth and fractal basins of attraction. *J. Sound Vib.* **135**, 453–475.

Soliman, M. S. & Thompson, J. M. T. 1991 Transient and steady state analysis of capsize phenomena. *Appl. Ocean Res.* **13**, 82–92.

Soliman, M. S. & Thompson, J. M. T. 1992 Global dynamics underlying sharp basin erosion in nonlinear driven oscillators. *Phys. Rev.* A. (In the press.)

Stewart, H. B. & Ueda, Y. 1991 Catastrophes with indeterminate outcome. *Proc. R. Soc. Lond.* A **432**, 113–123.

Thompson, J. M. T. 1989 Chaotic phenomena triggering the escape from a potential well. *Proc. R. Soc. Lond.* A **421**, 195–225.

Thompson, J. M. T. 1991 Transient basins: A new tool for designing ships against capsize. In *Proc. IUTAM Symp. Dynamics of Marine Vehicles & Structures in Waves* (ed. W. G. Price *et al.*), pp. 325–331. Amsterdam: Elsevier.

Thompson, J. M. T., Rainey, R. C. T. & Soliman, M. S. 1990 Ship stability criteria based on chaotic transients from incursive fractals. *Phil. Trans. R. Soc. Lond.* A **332**, 149–167.

Thompson, J. M. T. & Soliman, M. S. 1990 Fractal control boundaries of driven oscillators and their relevance to safe engineering design. *Proc. R. Soc. Lond.* A **428**, 1–13.

Thompson, J. M. T. & Soliman, M. S. 1991 Indeterminate jumps to resonance from a tangled saddle-node bifurcation. *Proc. R. Soc. Lond.* A **432**, 101–111.

Thompson J. M. T. & Stewart, H. B. 1986 *Nonlinear dynamics and chaos*. Chichester: Wiley.

PHILOSOPHICAL TRANSACTIONS OF THE ROYAL SOCIETY A MATHEMATICAL, PHYSICAL & ENGINEERING SCIENCES